

1,3,8-Triazaspiro[4.5]decane-2,4-diones as Efficacious Pan-Inhibitors of Hypoxia-Inducible Factor Prolyl Hydroxylase 1–3 (HIF PHD1–3) for the Treatment of Anemia

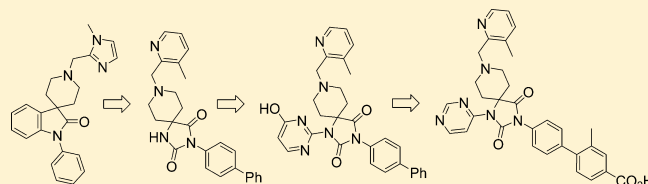
Petr Vachal,^{*,†} Shouwu Miao,[†] Joan M. Pierce,[†] Deodial Guiadeen,[†] Vincent J. Colandrea,[†] Matthew J. Wyvratt,[†] Scott P. Salowe,[‡] Lisa M. Sonatore,[‡] James A. Milligan,[§] Richard Hajdu,[§] Anantha Gollapudi,[§] Carol A. Keohane,[§] Russell B. Lingham,[§] Suzanne M. Mandala,[§] Julie A. DeMartino,[§] Xinchun Tong,^{||} Michael Wolff,^{||} Dietrich Steinhuebel,[⊥] Gerard R. Kieczkowski,[⊥] Fred J. Fleitz,[⊥] Kevin Chapman,[#] John Athanasopoulos,[#] Gregory Adam,[#] Can D. Akyuz,[▽] Dharendra K. Jena,[▽] Jeffrey W. Lusen,[#] Juncai Meng,[▽] Benjamin D. Stein,[▽] Lei Xia,[▽] Edward C. Sherer,[○] and Jeffrey J. Hale[†]

Departments of [†]Medicinal Chemistry, [‡]Infectious Diseases; [§]Immunology; ^{||}Drug Metabolism/Pharmacokinetics; [⊥]Process Research; [#]Target Validation; [▽]Information Technology; [○]Chemistry Modeling and Informatics. Merck Research Laboratories, Rahway, New Jersey 07065, United States

S Supporting Information

ABSTRACT: The discovery of 1,3,8-triazaspiro[4.5]decane-2,4-diones (spirohydantoin)s as a structural class of pan-inhibitors of the prolyl hydroxylase (PHD) family of enzymes for the treatment of anemia is described. The initial hit class, spirooxindoles, was identified through affinity selection mass spectrometry (AS-MS) and optimized for PHD2 inhibition and optimal PK/PD profile (short-acting PHDi inhibitors).

1,3,8-Triazaspiro[4.5]decane-2,4-diones (spirohydantoin)s were optimized as an advanced lead class derived from the original spiroindole hit. A new set of general conditions for C–N coupling, developed using a high-throughput experimentation (HTE) technique, enabled a full SAR analysis of the spirohydantoin)s. This rapid and directed SAR exploration has resulted in the first reported examples of hydantoin derivatives with good PK in preclinical species. Potassium channel off-target activity (hERG) was successfully eliminated through the systematic introduction of acidic functionality to the molecular structure. Undesired upregulation of alanine aminotransferase (ALT) liver enzymes was mitigated and a robust on-/off-target margin was achieved. Spirohydantoin)s represent a class of highly efficacious, short-acting PHD1–3 inhibitors causing a robust erythropoietin (EPO) upregulation in vivo in multiple preclinical species. This profile deems spirohydantoin)s as attractive short-acting PHDi inhibitors with the potential for treatment of anemia.



■ INTRODUCTION

Anemia, generally defined as a decrease in normal levels of red blood cells (RBCs) or/and hemoglobin (i.e., hemoglobin levels <12 g/dL), may be caused by a range of medical conditions, some of which are potentially very serious and carry significant risk factors. These include chronic kidney disease (CKD),¹ chemotherapy-induced anemia (CIA),² and anemia of chronic disease (ACD).^{3,4} Currently available treatments of anemia typically rely on intravenous (iv) administration of either RBCs or recombinant erythropoietin (rhEPO).⁵ While administration of the former tends to be complicated by undesired iron and RBC level fluctuations, the latter option represents an expensive treatment that makes it inaccessible to many patients.⁶ Furthermore, iv administration may cause additional adversity among patients because it often requires hospitalization. Discovery of a new, orally bioavailable, and economically viable alternative to combat anemia would most likely have a profound impact on the lives of this patient population.

It has been proposed that the RBC biosynthesis, clinically demonstrated to be stimulated by rhEPO iv therapy, may be

achieved by endogenous EPO upregulation through upregulation of hypoxia-inducible factor (HIF; Figure 1). HIF is a heterodimeric transcription factor biosynthesized from a constitutively expressed subunit HIF β and an oxygen-regulated subunit HIF α . HIF α is short-lived under oxygen-normal conditions and undergoes an oxidative degradation regulated by prolyl hydroxylases 1–3 (PHD1–3). It has been postulated that if PHD1–3 are downregulated, as they would naturally be under hypoxia conditions (e.g., at high altitudes), the oxidative degradation of HIF α should be impeded and thus the rate of biosynthesis of HIF amplified due to the higher concentration of rate-limiting HIF α , ultimately leading to EPO upregulation.⁷ This hypothesis is consistent with the recent outcome of Fibrogen's FG-2216 PhII clinical trial, supporting the exciting opportunity to pursue an orally bioavailable therapy, in principle significantly less expensive than the current treatments

Received: November 15, 2011

Published: February 27, 2012

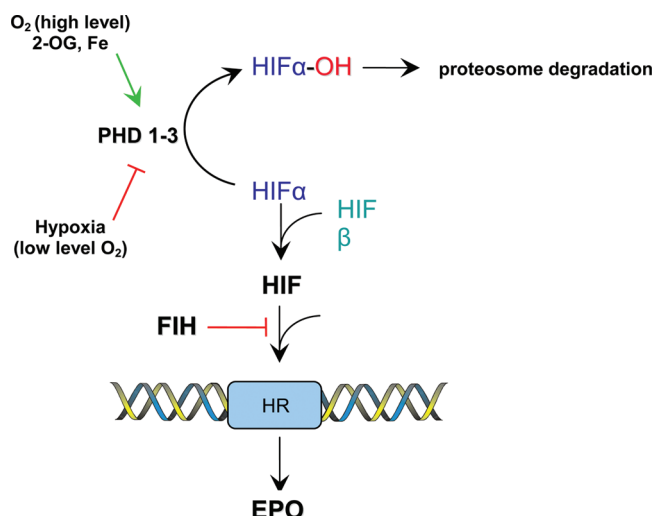


Figure 1. Rationale for PHD1–3 inhibition as potential mechanism for increasing RBC count through upregulation of EPO: impeding oxidative degradation of HIF α through PHD1–3 downregulation amplifies rate of HIF biosynthesis due to the higher concentration of rate-limiting HIF α , ultimately leading to upregulation of HIF and EPO.

and thus generally more accessible, for certain types of anemia.^{8–10}

The discovery efforts centered around one of the enzymes of the PHD family, PHD2. The enzyme had been successfully isolated and purified,¹¹ which allowed for the application of the high-throughput (HT) affinity selection mass spectrometry (AS-MS)¹² technique as the basis for the initial small molecule hit identification. Pure PHD2 enzyme was incubated with mixtures of hundreds of compounds per well. The resulting mixtures were treated using size exclusion techniques to discriminate unbound protein from potential protein–ligand complexes. Protein–ligand complexes were subsequently trapped and dissociated, yielding unbound compounds which were analyzed by mass spectrometry. AS-MS enabled a rapid screen of approximately 500000 molecules, yielding a prominent hit class of proprietary spiroindoles depicted in Figure 2.

RESULTS AND DISCUSSION

Representative examples of spirohydantoin AS-MS hits **3a–3j** were resynthesized and tested as discrete compounds in PHD2 in vitro binding assay.¹³ This exercise confirmed that the binding affinity, qualitatively observed by AS-MS, in fact translated quantitatively into PHD2 enzyme inhibition in the

0.4–8 μ M range in vitro (**3a–3j**, Table 1). While substituent R³ appeared sterically forgiving with respect to PHD2 inhibition because no significant difference was observed for hydrogen vs isopropyl (**3a** vs **3b**), both R¹ and R² groups appeared to have a significant impact on the in vitro inhibition. In addition to the SAR data shown in Table 1 for **3a–3j**, several hundred R¹ and R²-derivatives of **3**, presumably included in the initial 500000-member collection mixtures, did not qualitatively show binding affinity for PHD2 in the AS-MS screen (Figure 2). This fact is consistent with the importance of the R¹ and R² substituents and provides additional evidence for real SAR causality in the series. These observations warranted a systematic SAR investigation of the spiroindole hit series. A general research operation plan was established, described therein by means of the hierarchy of biological assays utilized for SAR optimization:¹³

- Primary in vitro screening assays
 - PHD1, PHD2, PHD3 inhibition binding assays (HT)
 - General counter screens, including hERG binding assay and CYP's inhibition assay (HT)
 - Project-specific counter screen: factor Inhibiting HIF (FIH)
- Primary in vivo pharmacodynamic (PD) screening assays (Figure 3)
 - Mouse pharmacodynamic erythropoietin determination (MoPED; medium throughput)
 - Single dose iv, EPO (in vivo efficacy)
 - Single dose po, reticulocyte readout
 - Multiple dose PD (rat, dog, rhesus monkey), RBC count
 - ALT (acute toxicity)
- Primary in vivo PK assays (mouse, rat, dog, rhesus monkey)

Initial SAR optimization of the AS-MS hits, confirmed independently as singleton compounds, focused predominantly on increasing the in vitro inhibition of a single PHD enzyme subtype, PHD2. This strategy was largely driven by the fact that the PHD2 binding assay was of significant throughput and that no substantial selectivity for other PHD subtypes was generally observed (or desired) for the discovery program. The synthetic scheme depicted in Table 1 allowed for a facile survey of R¹ and R². Substitution at R¹ proved to be restricted to a rather small number of closely related analogues. Out of over 100 diverse heterocyclic substituents investigated for this position (data not shown), only 2-pyridylmethyl (e.g., **3j**) and 1-methylimidazole-2-ylmethyl (e.g., **3h**) and a handful of structurally closely related analogues were associated with a significant in vitro

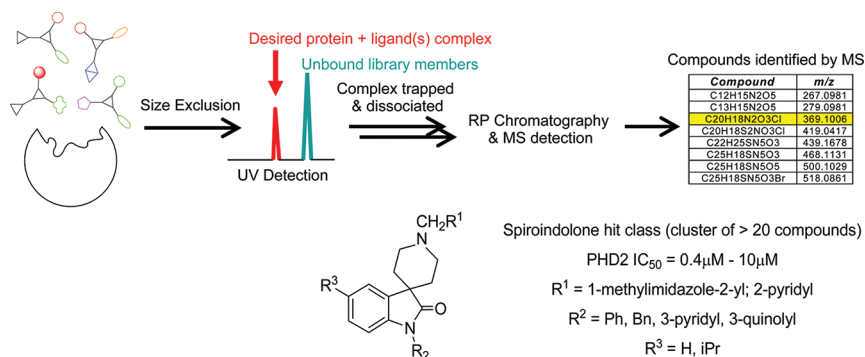


Figure 2. Identification of spiroindole hit series through AS-MS screening.

Table 1. In Vitro Inhibition of PHD2 by Spiroindole Derivatives; Initial SAR Work Up of the AS-MS Hit^a

| Compound | R ¹ - | R ² - | R ³ - | PHD2 IC ₅₀ (nM) | Compound | R ¹ - | R ² - | R ³ - | PHD2 IC ₅₀ (nM) |
|----------|------------------|------------------|------------------|----------------------------|----------|------------------|------------------|------------------|----------------------------|
| 3a | | | H- | 640 | 3u | | | H- | 3100 |
| 3b | | | iPr- | 680 | 3v | | | H- | 185 |
| 3c | | | H- | 6600 | 3w | | | H- | 840 |
| 3d | | | iPr- | 2200 | 3x | | | H- | 4700 |
| 3e | | | H- | 1200 | 3y | | | H- | 44 |
| 3f | | | H- | 1000 | 3z | | | H- | 6000 |
| 3g | | | iPr- | 7800 | 3aa | | | H- | 1200 |
| 3h | | | H- | 370 | 3bb | | | H- | 30 |
| 3i | | | H- | 2600 | 3cc | | | H- | 140 |
| 3j | | | H- | 790 | 3dd | | | H- | 52 |
| 3k | | | H- | >50000 | 3ee | | | H- | 6.8 |
| 3l | | | H- | >50000 | 3ff | | | H- | 4.0 |
| 3m | | | H- | >50000 | 3gg | | | H- | 7.8 |
| 3n | | | H- | >50000 | 3hh | | | H- | 11 |
| 3o | | | H- | 3040 | 3ii | | | Br- | 17 |
| 3p | | | H- | 440 | 3jj | | | CN- | 4.1 |
| 3q | | | H- | 15300 | 3kk | | | HOOC- | 0.7 |
| 3r | | | H- | >50000 | | | | | |
| 3s | | | H- | >50000 | | | | | |
| 3t | | | H- | >50000 | | | | | |

^aConditions: (a) LiHMDS, NMP then (ClCH₂CH₂)₂NBoc. (b1) (R² aromatic): R²X, CuI, K₂CO₃, MeNHCH₂CH₂NMe, MeCN, DMF. (b2) (R² aliphatic): R²X, NaH, DMF. (c) 4M HCl in dioxane. (d1) (R¹ aliphatic): R¹-¹³CCHO, NaBH(OAc)₃, MeCN. (d2) (R¹ aromatic): R¹X + conditions b1.

inhibition of PHD2. Any other investigated R¹ derivatives caused a significant decrease in the in vitro activity, typically by several

orders of magnitude. By way of exemplifying the narrow SAR of the R¹-position, it is noteworthy that seemingly close analogues of

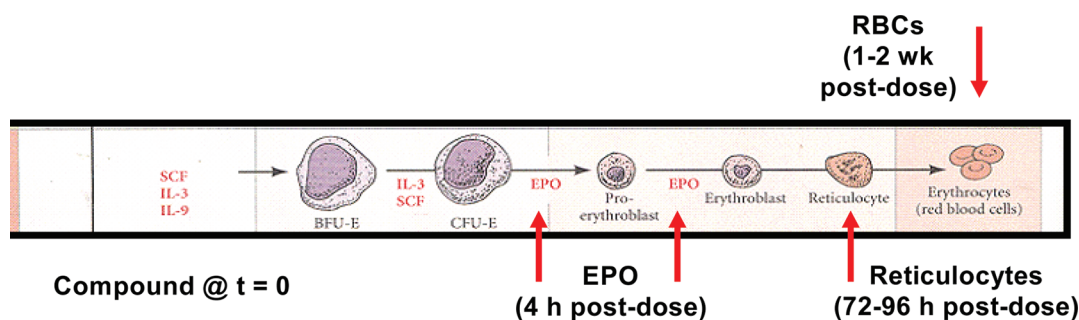


Figure 3. The principles for the primary in vivo PD assay: the investigated compound is administered at $t = 0$; in vivo PD readout based on EPO elevation (MOPED, iv single dose), reticulocyte elevation (po, single dose), or RBC count increase (chronic dosing).

3h and **3j** displayed no activity in vitro (compare **3h** vs **3k–l**, and **3j** vs **3m–o**, respectively). All compounds of the series suffered from poor PK in the rat and mouse, deeming it impossible to conclusively test the in vivo activity of the series in the primary PD model. It is noteworthy that **3p** and **3q**, for which some key physical properties were improved in vitro, did not provide a significantly better PK profile in vivo. Adding a methylene spacer to the R^1 substituent also proved important for the primary assay activity but at the same time represented a metabolic liability (the dealkylated spiroperidine was identified as one of the major metabolites in vitro). Attempts to alter the methylene spacer in an effort to improve the generally poor PK profile led to a complete loss of in vitro efficacy as evident from examples **3r–s**. An important leap forward for the R^1 substituent was accomplished through a comparison of the in vitro activity for close derivatives **3t** vs **3u**; while methylene substitution was detrimental to the in vitro activity in **3t**, 6-pyridine substitution was tolerated as evident by the measurable activity of **3u**. This observation led to the design and synthesis of **3v**, the most active compound of the series prepared thus far. Even though **3v** was still lacking robust in vivo PK in the rat, it proved to be relatively more stable in a side-by-side comparison with **3h** in the in vitro rat liver microsome (LM) incubation (35% vs <10% of parent remaining after 30 min, respectively), suggesting that the 2-pyridyl was a viable R^1 substituent alternative to the metabolically labile 1-methylimidazole-2-yl. Subsequent optimization of the 6-pyridyl position of **3v** improved neither in vitro activity nor liver microsome stability (**3v** vs e.g., **3w–x**), which validated 6-methyl-2-pyridylmethyl as the most promising R^1 pharmacophore.

Because of the synergistic nature of the SAR of R^1 and R^2 substituents, optimization of the R^2 substituent was conducted in parallel to the R^1 substituent optimization described previously. As such, one of the initial hits, **3h** (Table 1), had been selected as the starting point of the exercise. Approximately 50 aromatic, heteroaromatic, and aliphatic derivatives of **3h** were surveyed using the synthesis outlined in the scheme in Table 1, exemplified here by **3a–3h** and **3y–3bb**. In general, introduction of aromatic substituents provided stronger inhibition compared to their aliphatic (e.g., **3a** and **3y** vs **3c**) and heteroaromatic (e.g., **3a** vs **3z**, and **3h** vs **3y**) counterparts. The in vitro activity trend observed for a series of analogues **3z** > **3aa** > **3bb** suggested that the 4-substitution pattern of aromatic/heteroaromatic R^2 should provide an additional inhibition enhancement. Indeed, compounds **3cc–ee** provided significant improvement of in vitro inhibition compared to unsubstituted **3a**, yielding a strong PHD2 inhibition (**3ee**). Finally, combining optimized substituents R^1 (in **3v**) and R^2 (in **3ee**) produced analogue **3ff**, which showed 4 nM PHD2 inhibition in vitro.

While certainly encouraging from the in vitro inhibition stand point, compound **3ff** suffered from two major drawbacks: suboptimal PK in both rat and mouse (Table 2) and hERG off-target activity (binding hERG assay, $IC_{50} = 123$ nM). The former represented a very significant drawback as this prevented an in vivo proof-of-concept (POC) experiment, a potential ultimate validation of the series as viable specific PHD2 inhibitors. Several structurally related **3ff** R^2 analogues (Table 1, **3gg–hh**) and R^3 analogues (**3ii–kk**) were prepared in attempt to stabilize parts of the molecule identified as metabolic hot spots, however, none of the derivatives led to significant improvements in physical properties and metabolic stability (the later were generally prioritized by LM homogenate incubation in vitro followed by mouse/rat PK in vivo).

Because introduction of polar groups on the periphery of the **3ff** lead (substituents R^{1-3}) provided marginal improvement in the overall PK profile of the molecule, core altering changes of the spiroindole were pursued. First, the spiroindole moiety of **3ff** was replaced with aza-spiroindole; both 4- and 7-azaspiroindoles were synthesized (Table 2, **4a** and **4b**, respectively). While the 4-aza derivative **4a** failed to generate a PD response in vivo, the 7-aza analogue **4b** was weakly efficacious in the MOPED PD model, raising the EPO levels by approximately 800 ng/L after a single 50 mpk dose (Table 2). Albeit weak, the PD response represented the first evidence of statistically significant in vivo efficacy for the spiroindolone derivatives and thus provided a critical validation of the series. However, subsequent SAR optimization of **4b** by means of various pyridine, piperidine, and biphenyl substitutions did not result in any substantial improvement of the still suboptimal PD efficacy. More radical changes of the spiroindole core were envisioned with the intention of identifying the minimal pharmacophore and concomitantly reducing the lipophilicity of the lead. Examples of such derivatives, for which the level of the on-target in vitro inhibition was preserved, are depicted in Table 2 (**4c–g**). Derivatives **4c–e** proved nonefficacious in the primary PD assay. On the other hand, both examples of spirohydantoin analogues **4f–g** exhibited an in vivo efficacy at the level approximately equivalent to **4b**. Better physical properties and reduced molecular weight of **4f** were credited for similar efficacy despite the seemingly far inferior PK profile of **4f** compared vs **4b**. Furthermore, the presence of a free carboxylic acid in **4g** substantially improved the off-target profile of the series, informing us that the off-target activity may be derisked for a long-term developmental plan (e.g., compare hERG IC_{50} of 20 μ M vs 0.12 μ M for **4g** vs **4b**, respectively).

Improving the suboptimal in vivo efficacy and poor PK of the spirohydantoin **4f** derivatives became the central focus of the optimization effort. The analysis of hydantoins reported in the

Table 2. Attempting to Improve the PD Profile of **3ff** through Significant Changes of Its Spiroindole Core; R¹ = (3-methylpyridine-1-yl)methyl, R² = (4-phenylbenzene)-1-yl

| Compound | Structure | PHD2 IC ₅₀ (nM) | MOPED; ng/L (mpk dose) | PK (rat) |
|-----------------------|-----------|----------------------------|-------------------------------|---|
| 3ff | | 4.0 | <400 ^a (100mpk) | C _{max} = 79nM; Cl = 30mL/min/kg; Vdss = 8.2 L/kg; t _{1/2} = 3.0h AUC = 1.2uM.h; F = 11% |
| 4a | | 2.1 | <200 ^a (100mpk) | |
| 4b | | 1.6 | 800 ^b (50mpk) | C _{max} = 40nM; Cl = 59mL/min/kg; Vdss = 8.0L/kg; t _{1/2} = 1.9h AUC = 0.6uM.h; F = 0% |
| 4c | | 3.8 | <200 ^a (100mpk) | |
| 4d | | 98 | <200 ^a (100mpk) | |
| 4e | | 31 | <200 ^a (100mpk) | |
| 4f | | 8.9 | 900 ^b (100mpk) | C _{max} = 17nM; Cl = 275mL/min/kg; Vdss = 2.6L/kg; t _{1/2} = 0.12h AUC = 0.14uM.h; F = 42% |
| 4g^c | | 27 | 1200 ^b (100mpk) | C _{max} = 40nM; Cl = 11mL/min/kg; Vdss = 0.58L/kg; t _{1/2} = 1.1h AUC = 3.2uM.h; F = 14% |

^aNot statistically significant vs vehicle arm. ^bStatistically significant vs vehicle arm. ^cRacemate of a single diastereomer.

literature was consistent with our observation for **4f** that hydantoin is generally plagued with poor PK. However, virtually all of the literature examples of hydantoin happened to be either mono *N*-substituted or *N,N'*-disubstituted with at least one of the substituents being aliphatic. We hypothesized that *N,N'*-disubstituted hydantoin in which both *N*-substituents are either aromatic or heteroaromatic should be metabolically more stable. The hypothesis was tested on **6a**, an example of an *N'*-pyrimidine derivative of **4f**. The choice of this specific pyrimidine substituent was inspired by another program lead series in which it proved critical for PK properties enhancement (**5**, Figure 4).¹⁴ Indeed, the PK profile of *N,N'*-disubstituted **6a** was substantially improved compared to its

unsubstituted parent **4f**. An improved PK profile contributed to the dramatic boost of in vivo efficacy observed for **6a** (Figure 4, MOPED: 12000 ng/L at 100 mpk).¹⁵

The groundbreaking improvement of in vivo properties demonstrated by both the efficacy as well as favorable PK in multiple preclinical species (Figure 4, **6a**) warranted further SAR investigation of the *N'*-aryl substituent (Scheme 1, Ar group). However, reaction conditions suitable for the synthesis of **6a** via C–N coupling (**9** → **10**)¹⁶ failed to provide the desired analogues **6** for virtually all attempted aryl substituents. Because attempts to optimize step c of Scheme 1 in a traditional linear manner (one reaction at a time) failed to yield the desired intermediates **10**, a high-throughput experimentation

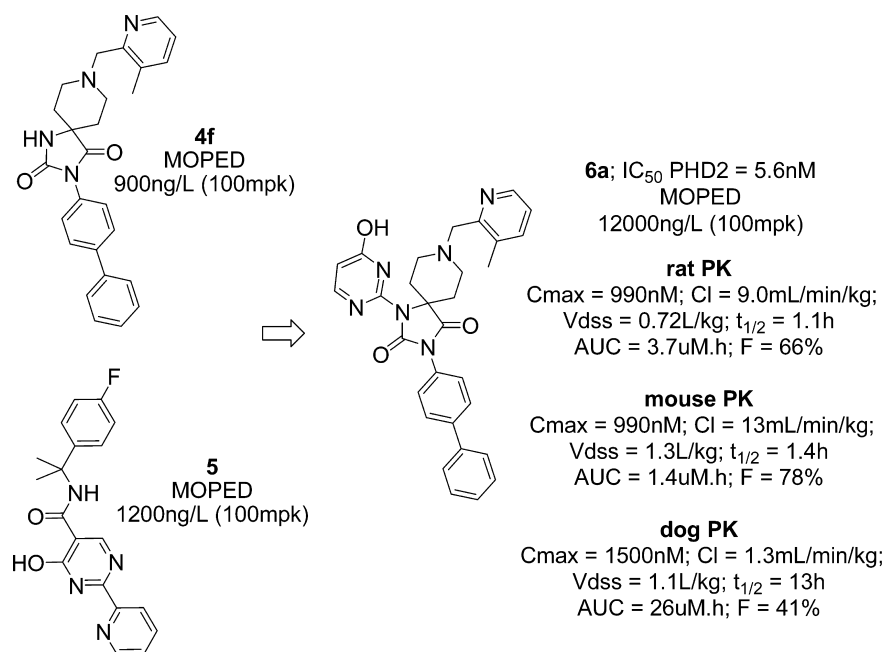
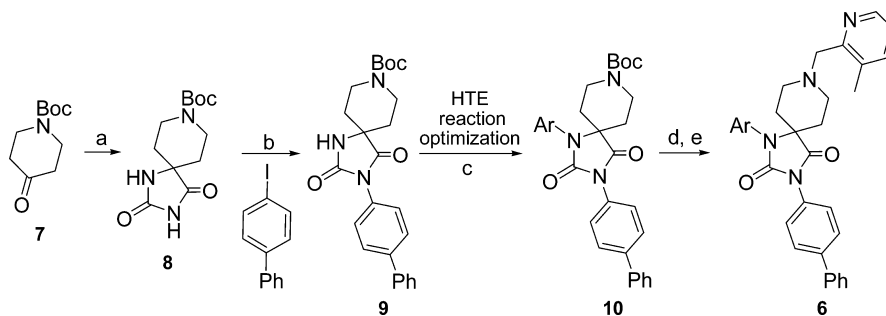


Figure 4. Improving the in vivo properties by merging the key structural features of two distinct program leads yielded a robust PD efficacy in MOPED model.

Scheme 1. High-Throughput Optimization of Reaction Conditions for *N'*-Aryl Coupling (Conditions c) Critical for the Detail SAR Optimization of Derivatives 6.^a



^aConditions: (a) KCN, (NH₄)₂CO₃ (95%); (b) CuI, K₂CO₃, MeNHCH₂CH₂NHMe, MeCN, DMF (78%); (c) reaction conditions optimized through HTE (Table 3): ArX (X = Br, I), CuI, TMHD, C₂CO₃, DMF, MeCN; (d) 4 M HCl in dioxane; (e) 3-methylpyridine-2-carboxaldehyde, NaBH(OAc)₃, MeCN.

Table 3. HTE Optimization of Reaction Conditions for C–N Coupling on Spirohydanotoin Core (Scheme 1; Step c: 9 → 10)^a

| ligand | DMEDA ^b | | DACH ^c | | proline | | <i>N,N</i> -diMe-glycine | | TMHD ^d | | 1,10-phenantroline | |
|----------------------------------|--------------------|-----------------|-------------------|-----------------|-----------------|-----------------|--------------------------|-----------------|-------------------|-----------------|--------------------|-----------------|
| | ArX/Base B | | | | | | | | | | | |
| | B1 ^e | B2 ^f | B1 ^e | B2 ^f | B1 ^e | B2 ^f | B1 ^e | B2 ^f | B1 ^e | B2 ^f | B1 ^e | B2 ^f |
| PhI | 32 | 24 | 1 | 5 | 0 | 5 | 1 | 46 | 57 | 98 | 2 | 3 |
| 2-iodopyridine | 33 | 95 | 9 | 65 | 1 | 13 | 1 | 78 | 45 | 100 | 64 | 100 |
| 3-iodopyridine | 3 | 5 | 1 | 0 | 1 | 6 | 1 | 1 | 19 | 71 | 2 | 2 |
| 2-I-pyridine-4-CO ₂ H | 1 | 24 | 0 | 1 | 0 | 0 | 0 | 1 | 1 | 94 | 0 | 73 |
| 2-bromopyrimidine | 0 | 0 | 0 | 0 | 0 | 1 | 0 | 0 | 2 | 47 | 4 | 41 |
| 2-iodothiophene | 0 | 3 | 0 | 0 | 0 | 2 | 0 | 17 | 2 | 36 | 0 | 3 |
| 3-iodothiophene | 2 | 33 | 0 | 0 | 0 | 6 | 0 | 56 | 20 | 90 | 2 | 11 |
| control (no ArX) | 0 | 0 | 0 | 0 | 0 | 0 | 0 | 0 | 0 | 0 | 0 | 0 |

^aGeneral screen conditions: 0.5 equiv of CuI vs 9, ligand/CuI ratio = 3.5/1, DMF/MeCN = 1/1, 110 °C, conversion after 20 h.

^bDimethylethylenediamine. ^c1,2-Diaminocyclohexane (trans, racemic). ^d1,1,6,6-Tetramethyl-3,5-heptadione. ^eB1 = K₃PO₄. ^fB2 = Cs₂CO₃.

(HTE) method¹⁷ was employed for reaction optimization. HTE enabled a rapid screen of all combinations of six ligands and two bases against seven model substrates in a single 96-well plate (Table 3). The object of the reaction optimization was to

overcome the inherent lack of reactivity, presumably due to the high steric hindrance of the spirohydanotoin *N*-coupling partner. Screening against a diverse subset of aryl halides was critical because our intention was to broadly investigate the SAR of 6a

Table 4. SAR Optimization of *N'*-Aryl Substituent of Spiroindolones 6

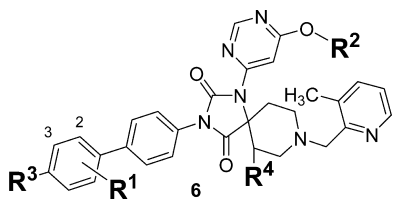
| Compound | Ar- | PHD1 PHD2 PHD3 IC ₅₀ (nM) | MED in MOPED; ng/L (dose; mpk) | PK (rat) |
|-----------|-----|--|--------------------------------------|--|
| 6a | | 1.8 3.0 20 | 6700 (50mpk) | C _{max} = 990nM; Cl = 9.0mL/min/kg; Vd _{ss} = 0.7L/kg; t _{1/2} = 1.1h; %F = 66 |
| 6b | | 1.4 4.3 97 | 1200 (100mpk) | |
| 6c | | 1.3 2.5 11 | 15000 (15mpk) | C _{max} = 950nM; Cl = 15mL/min/kg; Vd _{ss} = 1.0L/kg; t _{1/2} = 1.0h; %F = 37 |
| 6d | | 1.7 2.1 11 | 17000 (100mpk) | C _{max} = 101nM; Cl = 51mL/min/kg; Vd _{ss} = 2.1L/kg; t _{1/2} = 1.1; %F = 18 |
| 6e | | 1.4 4.3 97 | 1100 (15mpk) | C _{max} = 340nM; Cl = 35mL/min/kg; Vd _{ss} = 1.4L/kg; t _{1/2} = 0.5h; %F = 49 |
| 6f | | 1.4 3.4 44 | 1100 (15mpk) | C _{max} = 1300nM; Cl = 14mL/min/kg; Vd _{ss} = 0.9L/kg; t _{1/2} = 1.2h; %F = 39 |
| 6g | | 2.1 4.1 59 | 1100 (15mpk) | C _{max} = 300nM; Cl = 40mL/min/kg; Vd _{ss} = 1.1L/kg; t _{1/2} = 1.2h; %F = 58 |

derivatives. Finding conditions with a high coverage index (i.e., single set of conditions generally applicable to the synthesis of a variety of substrates) was more important than finding highly effective conditions only applicable to a limited number of substrates. Table 3 shows reaction conversion at 20 h as assayed by LCMS analysis normalized against an internal standard. It is notable that while some of the reaction conditions effectively converted **9** to the corresponding analogues **10** for some of the investigated aryl halide substrates, only a single set of conditions proved general for all of the aryl halides: the 1,1,6,6-tetramethyl-3,5-heptadione (TMHD) ligand with the cesium carbonate (B2) base (highlighted in Table 3). This result demonstrates the power of HTE, which yielded the general conditions for the conversion of **9** to **10** in a single parallel screen in less than 48 h total optimization time.

Armed with the general reaction conditions for the C–N coupling of aryl halides with spiroperidone **9**, approximately 30 aryl and heteroaryl (both 5- and 6-member heterocycl) analogues of **6** were synthesized according to Scheme 1. While most analogues exhibited promising in vitro enzyme inhibition, only a handful proved efficacious in vivo in the MOPED PD model, with the efficacy being strictly limited to pyridine derivatives (efficacious spiroperidones **6** are listed in Table 4). Several spirohydantoin **6** (**6c**, **6e–g**) exhibited a robust PD response after a single dose of 15 mpk, a remarkable efficacy considering the inherently short half-life ($t_{1/2}$ = 1–2 h) and a relatively high clearance for these molecules. It is noteworthy that prior to our work, there were no examples of orally bioavailable hydantoin derivatives reported in the literature. We concluded that the lack of favorable PK properties of previously reported hydantoin examples was consistent with the originally

proposed hypothesis that at least one of the hydantoin nitrogens was not substituted with an aromatic or heteroaromatic substituent, ultimately leading to metabolic liability of the molecule.¹⁸ The new C–N coupling reaction developed through HTE enabled us to access a completely new class of *N,N'*-bisarylsubstituted hydantoin derivatives **6** with good in vivo stability, a critical prerequisite for further development of the series, as well as establishing a proprietary intellectual property.

Once the spirohydantoin series was established as a viable lead class, rigorous off-target screening protocol was utilized to differentiate among a number of leading efficacious derivatives (**6c**, **6e–g**, Table 5). The series proved to be generally selective against standard off-targets (typically, PXR >50 μ M; CYP 3A4, 2C9, 2D6 >10 μ M; Cav1.2 >10 μ M) with the exception of the potassium channel (represented therein by the hERG binding assay). Carboxylic acid functionality was introduced into several suitable positions of the molecule, resulting in derivatives with variable PHD1–3 activity but generally clean hERG profiles. Carboxylic acid substitution of any available position of the pyrimidine ring proved detrimental to the primary in vitro activity (data not shown). On the other hand, both R³ and R⁴ carboxylic acid substitutions of **6** were tolerated, yielding derivatives **6h/6i** and **6j/6k**, respectively, with good in vitro profiles of which **6h** and **6k** also proved exceptionally efficacious in vivo even at a lower dose (MED = 5 mpk, iv). The 4-substitution pattern of **6k** was critical for the in vivo PD response as evidenced by complete loss of activity for positional isomers **6l** and **6m**. Two leading subclasses with developmental potential, represented by **6h** and **6k**, were differentiated based on their PK profile (Table 5^{a,b}): **6h** had a profile consistently

Table 5. SAR Optimization of Spiroindolones **6** for Optimal off-Target Profile (hERG Binding)


| 6 | R ¹ | R ² | R ³ | R ⁴ | PHDi IC ₅₀ (nM) | | | hERG binding (μM) | CYPs (μM) | MOPED ng/L (mpk) ↑ALT (mpk) |
|-----------------------|---------------------|----------------|-------------------|-------------------|----------------------------|-----|-----|-------------------|----------------------------------|--|
| | | | | | 1 | 2 | 3 | | | |
| 6c | H | H | H | H | 1.3 | 2.5 | 11 | 0.22 | 3A4 = 69 2C9 = 65 2D6 >100 | 26000 (50 iv) 15000 (15 iv) 910 (5 iv) 300 (1.5 iv) |
| 6h^a | H | H | H | CO ₂ H | | | | | | 9000 (15 iv) 1500 (5 iv) |
| 6i | H | Me | H | CO ₂ H | 1.1 | 0.4 | 3.5 | >30 | | 8000 (50 iv) 400 (15 iv) 200 (5 iv) |
| 6j | H | H | CO ₂ H | H | 1.1 | 1.1 | 7.2 | >30 | 3A4, 2C9, 2D6 >10 | 510 (50 iv) 210 (15 iv) |
| 6k^b | H | Me | CO ₂ H | H | 0.3 | 0.4 | 2.1 | 6.4 | 3A4, 2C9, 2D6 >50 | 14000 (15 iv) 1700 (5 iv) |
| | | | | | | | | | | ALT 6.1x (15 iv) ALT OK (5 iv) |
| 6l | 3-CO ₂ H | Me | H | H | 0.2 | 0.4 | 1.7 | 7.0 | 3A4, 2C9, 2D6 >50 | 260 (15 iv) |
| 6m | 2-CO ₂ H | Me | H | H | 8.2 | 5.0 | 95 | 2.4 | 3A4, 2C9, 2D6 >50 | 260 (50 iv) |
| 6n | 2-Cl | Me | CO ₂ H | H | 0.9 | 0.8 | 27 | >60 | 3A4, 2C9, 2D6 >50 | 11000 (100 iv) 120 (5 iv) |
| 6o | 3-Cl | Me | CO ₂ H | H | 1.2 | 1.0 | 8.4 | 5.7 | 3A4, 2C9, 2D6 >50 | 170 (15 iv) 120 (5 iv) |
| 6p | 2-F | Me | CO ₂ H | H | 0.4 | 0.4 | 3.6 | 54 | 3A4, 2C9, 2D6 >50 | 23000 (100 iv) 230 (5 iv) |
| 6q^c | 2-Me | Me | CO ₂ H | H | 0.2 | 0.2 | 1.9 | 13 | 3A4, 2C9, 2D6 >50 | 9700 (15 iv) 470 (5 iv) |
| | | | | | | | | | | ALT 3.8x (100 iv) ALT OK (50 iv) |
| 6r | 3-Me | Me | CO ₂ H | H | 0.3 | 0.5 | 5.8 | 23 | 3A4, 2C9, 2D6 >50 | 5400 (15 iv) 570 (5 iv) |
| | | | | | | | | | | ALT 5.1x (15 iv) |

^a**6h** rat PK: Cl_p = 1.2 mL/min/kg, Vd_{ss} = 0.34 L/kg, c_{max} = 63 nM, t_{1/2} = 3.6 h, %F = 4.3. Mouse PK (5 po): Cl_p = 0.9 mL/min/kg, Vd_{ss} = 0.4 L/kg, c_{max} = 300 nM, t_{1/2} = 2.1 h, %F = 7.1. ^b**6k** rat PK: Cl_p = 8.8 mL/min/kg, Vd_{ss} = 1.7 L/kg, c_{max} = 1900 nM, t_{1/2} = 2.6 h, %F = 92. Mouse PK (5 po): Cl_p = 1.2 mL/min/kg, Vd_{ss} = 0.4 L/kg, c_{max} = 6100 nM, t_{1/2} = 3.7 h, %F = 36; **6k** PPB (100%) m = 98.4, r = 98.2, d = 94.6, h = 99.4. ^c**6q** rat PK: Cl_p = 11.9 mL/min/kg, Vd_{ss} = 4.3 L/kg, c_{max} = 570 nM, t_{1/2} = 4.1, %F = 64; **6q** PPB (100%) m = 98.3, r = 98.4, d = 97.4, h = 99.7.

inferior to that of **6k** across multiple species (rat and mouse) deeming **6k** more suitable for further optimization.

Additional in vivo profiling of the leading derivative **6k** revealed an unexpected elevation in liver enzyme levels, ALT, at the higher iv dose experiments. Subsequent titrations established a 4–6-fold increase in ALT levels at 15, 50, and 100 mpk (no increase at 5 mpk), effectively defining a nonexistent window between the ALT No Observable Effect Level (NOEL) and the desired HIF-PHD MED for in vivo PD efficacy. Several closely related analogues of **6k** (**6l–r**) were prepared in an effort to probe the ALT elevation liability of the series. For most of these analogues, the MED in the PD assay

was shifted into the 50–100 mpk range, leaving only two examples, **6q–r**, efficacious at levels comparable to **6k** (5–15 mpk). While **6r** was also plagued by a lack of a measurable significant ALT NOEL/MOPED MED window, a statistically significant margin of at least 10-fold between the ALT elevation and MOPED efficacy could be established in case of **6q** (ALT NOEL = 50 mpk and MOPED MED = 5mpk, Table 5). This result warranted SAR optimization focused on increasing the window between the NOEL ALT and MOPED MED as well as improving the suboptimal PK profile of **6q** (Table 5, footnote c).

Because even relatively minor structural changes of the biphenyl portion of the **6k/6q** structure proved to have pronounced effects

on both the primary MOPED efficacy as well the undesired ALT elevation (Table 5), a detailed SAR analysis of the biphenyl pharmacophore was conducted including a broader range of structural variations in an attempt to expand the scope across a larger chemical space (Table 6 exemplifies the effort). Aliphatic replacements of the terminal aromatic ring proved detrimental to the PD efficacy as exemplified by comparing saturated **6s** (Table 6) to unsaturated **6c** (Table 4). Four- (**6t**), five- (**6u–aa**), and six-membered (**6bb–cc**) heterocyclic replacements of the terminal benzene ring, both *N*- (**6t**, **6v**) and *C*-linked (**6u**, **6w–cc**), did not provide any overall advantage when compared to **6q**. Because most of those derivatives lacked carboxylic acid functionality, methyl derivatives ($R^2 = \text{Me}$) generally also suffered from hERG off-target activity, while the more acidic (and more hERG selective) proteo derivatives ($R = \text{H}$) provided suboptimal PD efficacy compared to **6q**. Of all investigated substitutions, only **6x** proved weakly efficacious with MED at 50 mpk. Even heterocyclic analogues closely related to **6k** in which the carboxylic functionality was placed in the *pseudo*-para position lost essentially all in vivo efficacy (**6y–aa**). In vivo efficacy was maintained for some biaryl (**6ee–gg**) and fused (**6ii–kk**) R^1 substitutions, but the activity was limited to high dose experiments. Given the lack of a PD response at lower doses, it was impossible to reliably establish the margin of the desired PD efficacy over the undesired ALT up-regulation even for cases where no ALT increase was observed up to 100mpk (**6jj–kk**).

Because the structure diversity-oriented probe of the biphenyl subunit resulted in no improvement of the leading candidate **6q**, subsequent SAR investigation focused on relatively minor changes of the 4-position of the terminal benzene ring (**6ll–oo**) as well as substituting benzene with a pyridine ring (**6pp–rr**). Primary, secondary, and tertiary amides **6mm–oo** all proved efficacious in vivo, **6mm** even as low as 15 mpk, but at the same time **6mm** caused the undesired up-regulation of the ALT levels at the 50 mpk dose and thus provided a worse on-/off-target margin compared to **6q**. Introduction of nitrogen into one of the biphenyl benzene rings provided the desired improvement in the overall physical properties of the molecule as evidenced by the increased free fraction in plasma protein binding (PPB) across preclinical species (compare two pairs of direct N vs CH analogues, **6pp** vs **6k** and **6qq** vs **6q**, respectively, in footnotes to Tables 6 and 5). However, the free-fraction increase did not translate into an efficacy improvement in vivo (for most efficacious derivative **6pp**, MED = 50 mpk).

Methylpyridyl had been previously shown to be critical for both in vitro as well as in vivo efficacy for the spiroindolone series (Table 1), a trend subsequently verified for selected examples of the spirohydantoin series **6** (data not shown). At the same time, a detailed SAR optimization of the biphenyl subunit of the **6k/6q** lead series provided no significant improvement of in vivo efficacy in MOPED nor did it improve the undesired ALT off-target activity profile (Table 6). These two data sets essentially left the *N*-heteroaryl substituent as the only potential group to be modified with the aim to improve the ALT off-target activity. The aim was to maintain or improve the generally good on-target profile observed for a number of spirohydantoins **6**, such as **6k** and **6q**, and at the same time improve the ALT NOEL/MOPED MED margin (Table 7). Variation of the *N*-heteroaryl substituent provided a range of efficacy in the primary MOPED in vivo PD assay with four derivatives (**11a**, **11i**, **11k**, **11l**), exhibiting MED as low as 5 mpk. Of these four, two (**11i** and **11l**) did not cause ALT

elevation at the highest tested dose of 100 mpk, effectively providing the largest possible ALT NOEL/MOPED MED margin within the measured range ($\geq 20\times$). There were no significant off-target findings for **11i** and **11l**, which was consistent with the series being generally selective against Cav1.2 ($>20 \mu\text{M}$), PXR ($>30 \mu\text{M}$), CYPs induction, and hERG binding (Table 7).

While **11i** and **11l** were virtually indistinguishable based on their physicochemical properties, PPB free fraction, or PK, **11l** was superior to **11i** based on better selectivity against hERG and as such was selected for additional profiling in preclinical species. We reason that the relatively short half-life of **11l** represents the advantage of the spirohydantoin series for the HIF-PHD mechanism because only a very short-time inhibition of the PHDi is sufficient for HIF stabilization and further downstream EPO upregulation. Several in vitro experiments, including incubation with liver microsomes (Figure 5), correlate this favorable in vivo profile (observed in rat PK and mouse PD experiments) to human. This notion suggests that **11l** has the potential to be efficacious in humans, placing it in a unique position of a short-acting highly efficacious PHDi inhibitor. The combined characteristic profile of **11l** may significantly reduce the chance of finding unpredictable adverse effects (AEs) in the clinic, which are more likely to be caused by the longer half-life of other known PHDi inhibitors (i.e., shorter duration of action might result in comparable in vivo efficacy with a reduced risk of AEs).

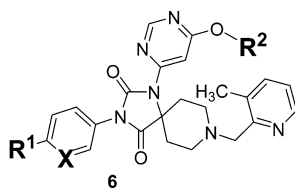
CONCLUSION

In conclusion, we developed a novel class of PHDi inhibitors exemplified by the highly efficacious, short-acting preclinical candidate **11l** (Figure 6). The initial spiroindolone program lead (hit class represented by **3a** in Figure 6) was discovered using the AS-MS screening methodology and systematically optimized for efficacy, off-target activity, and physical chemical properties. Judicious effort to identify the minimal pharmacophore of the spiroindolone led to the spirohydantoin class of compounds (exemplified by **4f** in Figure 6). For a thorough SAR optimization of the spirohydantoin series targeted at improving PK properties the need to prepare an array of unprecedented *N,N'*-diarylhantoins arose. The new chemical space was enabled by the discovery of an efficient, general C–N bond forming transformation through the use of HTE methodology. SAR optimization of the series for ALT elevation NOEL vs MOPED MED margin ultimately yielded **11l**. Given the complexity of the HIF-PHD mechanism of action for the treatment of anemia and possible AEs associated with the mechanism, we believe that **11l** represents a very promising clinical candidate due to its short acting PHDi inhibition resulting into robust downstream in vivo efficacy.

EXPERIMENTAL SECTION

General, Chemistry. Unless specified otherwise, all materials were purchased from commercial sources and used as received. ^1H and ^{13}C NMR spectra were recorded using a Bruker 400 MHz instruments. Preparative reverse phase liquid chromatography (RPHPLC) was performed using Waters MS directed purification system consisting of 2525 binary gradient pump, 2767 injector/collector, and 2996 PDA UV detector. Mobile phase: gradient of water and acetonitrile (each containing 0.1% TFA). Column: Waters Xterra (50 mm \times 3 mm, 3.5 μm packing material). The purity of **1–11** has been determined by HPLC analysis (electrospray positive ionization, Micromass ZQ single quadrupole)¹⁹ as $\geq 95\%$.

Table 6. SAR Optimization of the Biphenyl Portion of Spirohydantoin 6 for Optimal Desired Primary MOPEP PD and Undesired Off-Target Elevation of Liver Enzymes (ALT)



| 6 | R ¹ | X | R ² | PHDi IC ₅₀ (nM) | | | hERG binding (μ M) | CYPs (μ M) | MOPED ng/L (mpk) ↑ALT (mpk) |
|------------------|----------------|----|----------------|-------------------------------|-----|-----|-------------------------------|---------------------------------|---|
| | | | | 1 | 2 | 3 | | | |
| 6s | | CH | H | 1.9 | 5.0 | 120 | 1.0 | 3A4 = 40 2C9, 2D6 >50 | 170 (50iv) |
| 6t | | CH | H | 17 | 31 | 61 | 27 | 3A4, 2C9, 2D6 >50 | 170 (50 iv) |
| 6u | | CH | H | 11 | 11 | 340 | 7.7 | 3A4, 2C9, 2D6 >50 | 200 (50 iv) |
| 6v | | CH | H | 38 | 76 | 320 | 9.0 | 3A4, 2C9, 2D6 >50 | 200 (50 iv) |
| 6w | | CH | H | 4.5 | 9.3 | 76 | 22 | 3A4, 2C9, 2D6 >50 | 73 (50 iv) |
| 6x | | CH | H | 0.4 | 0.9 | 5.9 | 0.95 | 3A4, 2C9, 2D6 >50 | 2800 (50 iv) 330 (15 iv) |
| 6y | | CH | Me | 0.3 | 0.6 | 2.0 | 12 | 3A4, 2C9, 2D6 >50 | 930 (50 iv) 130 (15 iv) |
| 6z | | CH | Me | 0.8 | 2.8 | 6.4 | 8.0 | 3A4, 2C9, 2D6 >50 | 200 (50 iv) |
| 6aa | | CH | Me | 5.5 | 4.9 | 38 | >60 | 3A4, 2C9, 2D6 >50 | 320 (50 iv) |
| 6bb | | CH | H | 5.6 | 14 | 61 | <i>Nd</i> | <i>nd</i> | 540 (50 iv) 180 (15 iv) |
| 6cc | | CH | H | 2.0 | 3.9 | 21 | >60 | 3A4, 2C9, 2D6 >50 | 130 (50 iv) |
| 6dd | | CH | Me | 6.0 | 5.4 | 130 | 2.0 | 3A4, 2C9, 2D6 >50 | 720 (50 iv) 140 (15 iv) |
| 6ee | | CH | H | 0.2 | 0.2 | 3.5 | 8.1 | 3A4, 2C9, 2D6 >50 | 11000 (100 iv) 110 (5 iv) |
| 6ff ^d | | CH | H | 0.5 | 0.6 | 9.8 | 13 | 3A4, 2C9, 2D6 >50 | 29000 (100 iv) 310 (5 iv) ALT OK (100 iv) |
| 6gg | | CH | Me | 0.8 | 1.1 | 38 | 17 | 3A4, 2C9, 2D6 >50 | 20000 (100 iv) 140 (5 iv) ALT OK (100 iv) |
| 6hh | | CH | Me | 2.1 | 2.0 | 48 | 0.72 | 3A4, 2C9, 2D6 >50 | 120 (25 iv) |
| 6ii | | CH | Me | 2.3 | 2.3 | 47 | 4.7 | 3A4, 2D6 >50, 2C9 = 25 | 9400 (100 iv) 180 (5 iv) |
| 6jj | | CH | Me | 1.8 | 1.5 | 24 | 15 | 3A4 = 18 2C9 = 30 2D6 >50 | 5500 (100 iv) 140 (5 iv) |
| 6kk | | CH | H | 0.2 | 0.2 | 1.6 | 1.5 | 3A4, 2C9, 2D6 >50 | 19000 (100 iv) 230 (15 iv) ALT 3.2x (100iv) |

Table 6. continued

| 6 | R ¹ | X | R ² | PHDi IC ₅₀ (nM) | | | hERG binding | CYPs (μ M) | MOPED ng/L (mpk) |
|------------------|----------------|----|----------------|-------------------------------|-----|----|-----------------|----------------------------------|--|
| 6ll | | CH | Me | 1.1 | 1.6 | 17 | 0.37 | 3A4, 2D6 >50, 2C9 = 10 | 230 (15 iv) |
| 6mm | | CH | Me | 0.7 | 0.8 | 15 | 0.65 | 3A4, 2C9, 2D6 >50 | 2100 (15 iv) 270 (5 iv) ALT 6.6x (50 iv) ALT OK (15 iv) |
| 6nn | | CH | Me | 0.3 | 0.5 | 14 | 8.5 | 3A4 >50 2C9 = 44 2D6 = 2.7 | 28000 (100 iv) 170 (5 iv) |
| 6oo | | CH | Me | 3.7 | 4.7 | 49 | 8.9 | 3A4, 2C9 >50, 2D6 = 8.9 | 6500 (50 iv) 140 (5 iv) |
| 6pp ^b | | N | Me | 1.1 | 1.6 | 20 | 46 | 3A4, 2C9, 2D6 >50 | 7800 (50 iv) 500 (15 iv) 105 (5 iv) ALT OK (50 iv) |
| 6qq ^c | | N | Me | 1.6 | 1.9 | 36 | 7.1 | 3A4, 2C9, 2D6 >50 | 20000 (100 iv) 210 (5 iv) ALT 2.8x (100 iv) |
| 6rr | | N | H | 0.5 | 0.6 | 26 | 20 | 3A4, 2C9, 2D6 >50 | 130 (50 iv) |

^a6ff PPB (100%): $m = 94.8$, $r = 99.2$, $d = 98.3$, $h = 97.3$. ^b6pp PPB (100%): $m = 93.8$, $r = 96.1$, $d = 90.6$, $h = 97.8$. ^c6qq PPB (100%): $m = 88.5$, $r = 92.9$, $d = 83.0$, $h = 98.7$.

Preparation of 3ff (oxindole \rightarrow 1a \rightarrow 2ff \rightarrow 3ff; Scheme in Table 1) represents a typical procedure used for the synthesis of spiroindoles 3a–3kk. Preparation of 6c (8 \rightarrow 9 \rightarrow 10c \rightarrow 6c; Scheme 1) represents a typical procedure used for the synthesis of spiroindoles 4f, 4g, 6a–rr, 11a–11m.

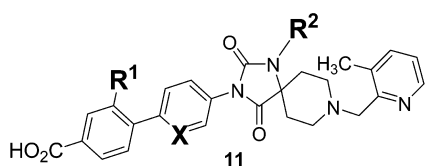
tert-Butyl 2-Oxo-1,2-dihydro-1'-H-spiro[indole-3,4'-piperidine]-1'-carboxylate (1a, R³ = H). Oxindole (44 g, 330 mmol) was dissolved in diemthoxyethane (DME, 880 mL), and the solution was cooled to -78 °C. A solution of LiHMDS/DME (550 mL, prepared by dissolving 246 g of 97% of LiHMDS in 750 mL of DME) was added over 40 min, maintaining an internal temperature of <-55 °C. The suspension was warmed to -30 °C over 30 min, and a solution of *N*-Boc-bis(2-chloroethyl)amine²⁰ (92.1 g, 380 mmol) in DME (120 mL) was added. The reaction mixture was allowed to warm to room temperature and stirred 18 h. An additional 280 mL of the LiHMDS solution was added in portions over 2 days. The reaction mixture was poured into 1.7 L of 2N HCl and ice and aged for 1 h. The mixture was diluted with 2 L of ether/hexanes (1/1) and the layers separated. The organic layer was washed with water (1 L), saturated sodium bicarbonate solution (1.5 L), and brine (0.5 L). The organic layer was dried over MgSO₄ and treated with Darco G-60. The mixture was filtered through MgSO₄, and the filtrate was concentrated to slurry. The slurry was filtered and the cake washed with hexanes affording 80.5 g (81%) of 1a as a white solid. LCMS: 2.4 min, m/z (M-BocH)⁺ = 203.2.

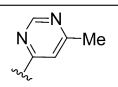
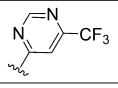
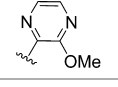
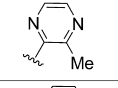
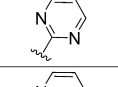
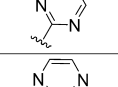
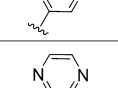
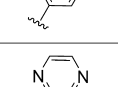
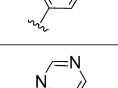
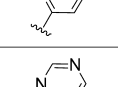
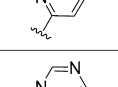
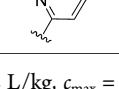
tert-Butyl 2-Oxo-1-(biphenyl-4-yl)-1,2-dihydro-1'-H-spiro[indole-3,4'-piperidine]-1'-carboxylate (2ff, R² = H, R³ = 4-biphenyl). In an oven-dried flask, 1a (2.8 g, 9.26 mmol) and 4-iodobiphenyl (3.37 g, 12.04 mmol) were dissolved in acetonitrile (100 mL), and the mixture was degassed with stream of nitrogen through the solution at 40 °C for 20 min. Anhydrous potassium carbonate (3.84 g, 27.8 mmol), copper(I) iodide (0.441 g, 2.315 mmol), and *N,N'*-dimethylethylenediamine (0.204 g, 2.315 mmol) were added sequentially, and the resulting reaction mixture was heated to 80 °C for 15 h under nitrogen and then cooled to

room temperature. The crude mixture was diluted with ethyl acetate and washed with 0.1 M HCl solution, dried over sodium sulfate, filtered, and concentrated. Further purification of the desired product was accomplished by column chromatography on silica gel, eluting with a gradient of ethyl acetate in hexanes 0–40%/1.3 L, yielding 3.1 g (74%) of 2ff as a white solid. LCMS: 4.10 min, m/z (M-BocH)⁺ = 355.1.

1-(Biphenyl-4-yl)-1'-[(3-methylpyridin-2-yl)methyl]spiro[indole-3,4'-piperidin]-2-(1H)-one (3ff). Hydrogen chloride (4 M) solution in dioxane (60 mL, 240 mmol) was added to 2ff (3 g, 6.60 mmol) via syringe in one portion, and the resulting mixture was stirred at room temperature for 1 h, concentrated to an approximate volume of 30 mL, and cooled to 10 °C. Solids were collected by filtration, rinsed with 10 mL of dioxane, and dried in a desiccator to yield deprotected amine intermediate as a white solid (6.0 mmol). LCMS 2.92 min, m/z (MH)⁺ = 355.1. To a solution of the amine intermediate (6.0 mmol) in methylene chloride (120 mL), 3-methylpyridine-2-carboxaldehyde (6.6 mmol), and sodium triacetoxyborohydride (18 mmol) were added sequentially, and the resulting mixture was stirred at ambient temperature for 2 h. Methanol (60 mL) was added, and the resulting mixture stirred at room temperature for 5 min and concentrated. The final purification was accomplished by preparative reverse phase HPLC to yield 2.9 g (77%) of 3ff a white trifluoroacetic acid salt. ¹H NMR (500 MHz, CD₃OD): 2.32 (m, 2H), 2.41 (s, 3H), 2.57 (m, 2H), 3.75 (m, 2H), 4.09 (m, 2H), 4.70 (s, 2H), 6.95 (d, $J = 8.2$ Hz, 1H), 7.22 (t, $J = 5.5$ Hz, 1H), 7.34 (t, $J = 5.5$ Hz, 1H), 7.38 (m, 1H), 7.54 (m, 2H), 7.63 (d, $J = 9.2$ Hz, 2H), 7.74 (d, $J = 9.6$ Hz, 2H), 7.85 (d, $J = 9.2$ Hz, 2H), 7.90 (d, $J = 7.8$ Hz, 1H), 8.18 (d, $J = 7.8$ Hz, 2H), 8.78 (d, $J = 3.2$ Hz, 1H). LCMS: 3.15 min, m/z (MH)⁺ = 460.1.

tert-Butyl 2,4-Dioxo-3-(biphenyl-4-yl)-1,3,8-triazaspiro[4.5]-decane-8-carboxylate (9). A solution of 8²¹ (23.8 mmol) and 4-iodobiphenyl (22.6 mmol) in acetonitrile (80 mL) and DMF (80 mL) was degassed with a stream of nitrogen for 15 min. *N,N'*-Dimethylethylenediamine (5.94 mmol), copper(I) iodide (5.94 mmol), and

Table 7. SAR Optimization of the *N*-Heteroaryl Portion of Spirohydantoin 6/11 for Optimal Desired Primary MOPED PD and Undesired Off-Target Elevation of Liver Enzymes (ALT)


| 11 | R ¹ | X | R ² | PHDi IC ₅₀ (nM) | | | hERG binding (μM) | CYPs (μM) | MOPED ng/L (mpk) ↑ALT (mpk) | PPB (100%) |
|------------------|----------------|----|---|-------------------------------|-----|-----|-------------------------|-------------------------------------|---|--|
| | | | | 1 | 2 | 3 | | | | |
| 11a | Me | CH |  | 0.2 | 0.2 | 3.2 | 38 | 3A4, 2C9, 2D6 >50 | 11000 (15 iv) 1000 (5 iv) ALT 3.0x (100 iv) | |
| 11b | Me | CH |  | 0.4 | 0.5 | 4.1 | 21 | 3A4, 2C9, 2D6 >50 | 9900 (15 iv) 350 (5 iv) ALT 2.1x (100 iv) | |
| 11c | Me | CH |  | 0.3 | 0.2 | 7.7 | 22 | 3A4, 2C9, 2D6 >50 | 4800 (15 iv) 180 (5 iv) ALT OK (100 iv) | |
| 11d | Me | CH |  | 0.2 | 0.2 | 2.0 | 1.4 | 3A4, 2C8, 2D6 >50 2C8 = 27 | 27000 (100 iv) 485 (15 iv) 97 (5 iv) ALT OK (100 iv) | |
| 11e | Me | CH |  | 0.3 | 0.2 | 4.9 | 7.8 | 3A4, 2C8, 2C9, 2D6 >50 | 18000 (50 iv) 4200 (15 iv) 220 (5 iv) ALT OK (50 iv) | |
| 11f ^a | H | CH |  | 1.2 | 0.8 | 10 | 19 | 3A4, 2C9, 2D6 >10 | 6000 (50 iv) 1300 (15 iv) | |
| 11g | Me | CH |  | 0.3 | 0.4 | 2.9 | 23 | 3A4, 2C9, 2D6 >50 | 1600 (50 iv) 260 (15 iv) ALT OK (50 iv) | |
| 11h | H | CH |  | 0.4 | 0.4 | 4.8 | 16 | 3A4, 2C9, 2D6 >50 | 1600 (50 iv) 280 (15 iv) | |
| 11i ^b | Me | CH |  | 0.2 | 0.2 | 0.8 | 7.2 | 3A4, 2C9, 2D6 >50 | 28000 (100 iv) 580 (5 iv) ALT OK (100 iv) | m = 85.8 r = 95.0 d = 93.8 h = 95.4 |
| 11j | Me | N |  | 1.0 | 1.0 | 43 | 2.5 | 3A4, 2C9, 2D6 >50 | 1100 (100 iv) 130 (5 iv) | m = 62.4 r = 78.8 d = 75.0 h = 90.0 |
| 11k ^c | H | CH |  | 0.3 | 0.2 | 2.1 | 31 | 3A4, 2C9, 2D6 >50 | 6400 (15 iv) 540 (5 iv) ALT OK (50 iv) | m = 96.9 r = 98.1 d = 92.5 h = 98.4 |
| 11l ^d | Me | CH |  | 0.2 | 0.2 | 1.6 | 22 | 3A4, 2C9, 2D6 >50 | 19000 (100 iv) 760 (5 iv) ALT OK (100 iv) | m = 95.6 r = 97.9 d = 94.3 h = 96.0 |
| 11m | Me | N |  | 1.0 | 0.8 | 22 | n/a | n/a | 930 (50 iv) 160 (15 iv) | |

^a11f rat PK: Cl_p = 51 min/mL/kg, Vd_{ss} = 2.2 L/kg, c_{max} = 100 nM, t_{1/2} = 1.1 h, %F = 18. ^b11i rat PK: Cl_p = 22 min/mL/kg, Vd_{ss} = 1.6 L/kg, c_{max} = 390 nM, t_{1/2} = 1.5 h, %F = 29. ^c11k rat PK: Cl_p = 16 min/mL/kg, Vd_{ss} = 2.0 L/kg, c_{max} = 580 nM, t_{1/2} = 2.2 h, %F = 8. ^d11l rat PK: Cl_p = 34 min/mL/kg, Vd_{ss} = 1.9 L/kg, c_{max} = 390 nM, t_{1/2} = 1.1 h, %F = 47.

potassium carbonate (71.3 mmol) were added sequentially. The resulting mixture was heated to 85 °C for 15 h, cooled to room temperature, and combined with ethyl acetate (300 mL) and water (300 mL). The organic layer was separated and washed with water (2 × 300 mL), dried over sodium sulfate, and concentrated. Purification by column chromatography on silica gel, eluted with a gradient of 0–100% hexanes in ethyl acetate, yielded 8.3 g (83%) of **9c** as a white solid. LCMS: 3.21 min, *m/z* (MH-Boc)⁺ = 321.0.

tert-Butyl 3-(Biphenyl-4-yl)-1-(6-methoxypyrimidin-4-yl)-2,4-dioxo-1,3,8-triazaspiro[4.5]decane-8-carboxylate (**10c**, Ar = 4-methoxypyrimidine-2-yl). A solution of **9** (10 mmol), 2-iodo-4-methoxypyrimidine (30 mmol) in acetonitrile (20 mL), and DMF (20 mL) was degassed with

a stream of nitrogen for 15 min. 2,2,6,6-Tetramethyl-3,5-heptadion (10 mmol), copper(I) iodide (10 mmol), and cesium carbonate (50 mmol) were added sequentially, and the resulting mixture was heated to 85 °C for 15 h and allowed to cool to room temperature. The mixture was combined with ethyl acetate (300 mL) and water (300 mL). The organic layer was separated and washed with water (2 × 300 mL), dried over sodium sulfate, and concentrated. Purification by preparative HPLC yielded 5.0 g (78%) of **10c** as a white salt of trifluoroacetic acid. LCMS: 4.21 min, *m/z* (MH-Boc)⁺ = 430.2.

3-(Biphenyl-4-yl)-8-[(3-methylpyridin-2-yl)methyl]-1-(6-hydroxypyrimidin-4-yl)-1,3,8-triazaspiro[4.5]decane-2,4-dione (**6c**). Boc Deprotection. A 4 M solution of hydrogen chloride in dioxane (60 mL, 240 mmol)

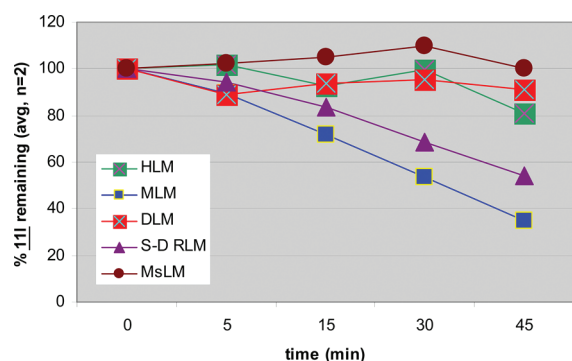


Figure 5. Incubation of **111** with liver microsomes across species correlates well rat PK and mouse PD profile to human in vitro.

was added to **10c** (6 mmol) via syringe. The resulting mixture was stirred at room temperature for 1 h, concentrated to an approximate volume of 30 mL, and cooled to 10 °C. Deprotected amine was isolated as a white solid by filtration, rinsed with 10 mL of dioxane, and dried in desiccator and used in the subsequent step without purification.

Reductive Amination. The deprotected amine (4 mmol) was dissolved in methylene chloride (40 mL). 3-Methylpyridine-2-carboxaldehyde (5 mmol) and sodium triacetoxyborohydride (20 mmol) were added to the solution sequentially. The resulting mixture was stirred at room temperature for 2 h. Methanol (20 mL) was added, and the resulting mixture was stirred at ambient temperature for 5 min and then concentrated. The purification was accomplished by preparative reverse phase HPLC yielding 2.4 g (93%) of *O*-methyl-**6c** as a white salt of trifluoroacetic acid. ¹H NMR (CDCl₃): δ = 2.03–2.15 (m, 4H), 2.03 (s, 3H), 3.53–4.30 (m, 6H), 4.06 (s, 3H), 6.60–8.49 (m, 14H). LCMS: 1.71 min, *m/z* (MH)⁺ = 535.

Demethylation. The *O*-methyl-**6c** (3.6 mmol) was combined with 1 M aqueous solution of hydrochloric acid (20 mL), and the resulting mixture was refluxed in a sealed tube for 8 h and concentrated. The final purification was accomplished by preparative reverse phase HPLC, yielding 2.0 g (89%) of **6c** as a white salt of trifluoroacetic acid. ¹H NMR (CDCl₃): δ = 1.96 (s, 3H), 2.24 (m, 2H), 2.34 (m, 2H), 3.84 (m, 2H), 3.92 (m, 2H), 4.48 (s, 2H), 6.18 (d, 1H, *J* = 6.6 Hz), 7.24–7.87 (m, 12H), 8.43 (d, 1H, *J* = 4.3 Hz). LCMS: 1.60 min, *m/z* (MH)⁺ = 521.

2-Methyl-4'-((3-methylpyridin-2-yl)methyl)-2,4-dioxo-1-(pyrimidin-4-yl)-1,3,8-triazaspiro[4.5]decan-3-yl)-[1,1'-biphenyl]-4-carboxylic acid (**111**) was prepared according to the general procedure described for **6c** (using 4-iodopyrimidine as the ArI) and isolated as a white solid of trifluoroacetic acid; **111**. ¹H NMR (CD₃OD): δ = 2.42 (s, 3H), 2.45 (m, 2H), 3.80 (m, 2H), 3.80–3.94 (m, 2H), 4.04–4.10 (m, 2H), 4.76 (s, 2H), 7.37 (m, 1H), 7.64 (d, *J* = 8.5 Hz, 2H), 7.74 (d, *J* = 7.6 Hz, 1H), 7.79 (d, *J* = 8.5 Hz, 2H), 7.86 (d, *J* = 8.5 Hz, 2H), 8.14 (d, *J* = 8.3 Hz, 2H), 8.46 (m, 1H), 8.54 (d, *J* = 4.7 Hz, 1H), 8.74 (d, *J* = 5.9 Hz, 1H), 9.06 (s, 1H). LCMS: 1.54 min, *m/z* (MH)⁺ = 549.3.

In Vitro Assay for HIF-PHD2. Catalytic activity represents a general procedure used for the determination of HIF-PHD catalytic activity for each of the three subtypes, HIF-PHD1–3: To each well of a 96-well plate was added 1 μL of test compound in DMSO and 20 μL of assay buffer (50 mM Tris pH 7.4/0.01% Tween-20/0.1 mg/mL bovine serum albumin/10 μM ferrous sulfate/1 mM sodium ascorbate/20 μg/mL catalase) containing 0.15 μg/mL FLAG-tagged full length PHD2 expressed in and purified from baculovirus-infected Sf9 cells. After a 30 min preincubation at room temperature, the enzymatic reactions were initiated by the addition of 4 μL of substrates (final concentrations of 0.2 μM 2-oxoglutarate and 0.5 μM HIF-1α peptide biotinyl-DLDLEMLAPYIPMDDDFQL). After 2 h at room temperature, the reactions were terminated and signals were developed by the addition of a 25 μL quench/detection mix to a final concentration of 1 mM *ortho*-phenanthroline, 0.1 mM EDTA, 0.5 nM anti-(His)₆ LANCE reagent (Perkin-Elmer Life Sciences), 100 nM AF647-labeled streptavidin (Invitrogen), and 2 μg/mL (His)₆-VHL complex.²² The ratio of time-resolved fluorescence signals at 665 and 620 nm was determined, and percent inhibition was calculated relative to an uninhibited control sample run in parallel.

MoPED (Mouse Plasma Erythropoietin Determination).

Compounds are formulated in cyclodextrin. Mice (C57Bl/6, *n* = 3) were dosed iv in a volume of 0.2 mL. After 4 h, blood was obtained via cardiac puncture upon euthanasia with CO₂. Plasma was stored at –80 °C and assayed the following day for Epo/VEGF. Results were compared to vehicle dosed controls.

Reticulocytes (Days 3 and 4 Post PO Dose). Compounds were formulated in cyclodextrin. Mice (C57Bl/6, *n* = 10) were dosed PO in a volume of 0.2 mL. On days 3 and 4 postdose, blood was obtained from five mice via cardiac puncture upon euthanasia with CO₂. Blood was analyzed for reticulocytes by FACS. Results were compared to vehicle dosed controls, and the assay was quality controlled by inclusion of a positive control compound, dosed at 15 mg/kg.

■ ASSOCIATED CONTENT

📄 Supporting Information

Full description of biological assays, characterization of compounds **3a–3kk**, **4a–g**, **6a–rr**, **11a–11m**, and synthetic procedures thereof as well as experimental details for the HTE optimization of C–N coupling (step c of Scheme 1). This material is available free of charge via the Internet at <http://pubs.acs.org>.

■ AUTHOR INFORMATION

Corresponding Author

*Phone: +1-732-594-6624. Fax: +1-732-594-9464. E-mail: petr_vachal@merck.com. Address: Merck Research Laboratories, RY123-2309, Rahway, NJ 07065, USA.

Notes

The authors declare no competing financial interest.

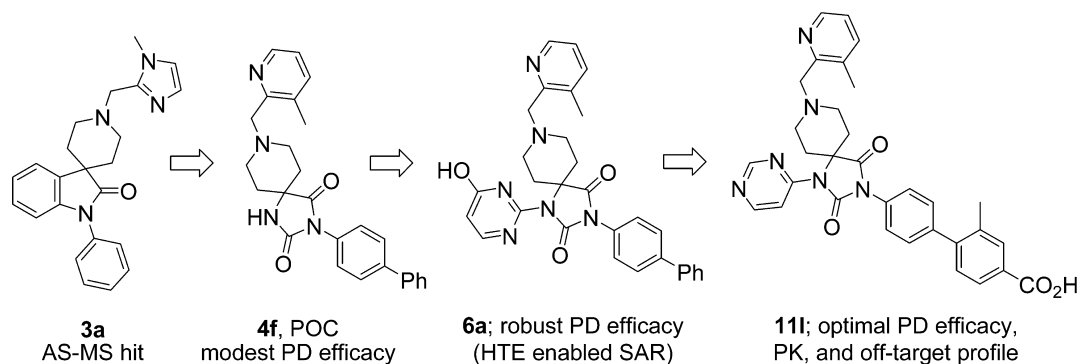


Figure 6. Overview of the discovery of a novel class of PHD2 inhibitors exemplified by highly efficacious, short-acting leading preclinical candidate **111**.

■ ABBREVIATIONS USED

PHD, prolyl hydroxylase; AS-MS, affinity selection mass spectrometry; HT, high-throughput; HTE, high-throughput experimentation; PK, pharmacokinetics; Kv11.1, potassium channel gene; hERG, human ether-à-go-go related gene; ALT, alanine aminotransferase; EPO, erythropoietin; RBC, red blood cell; CKD, chronic kidney disease; CIA, chemotherapy-induced anemia; ACD, anemia of chronic disease; iv, intravenous; HIF, hypoxia-inducible factor; FIH, factor inhibiting hypoxia-inducible factor; PD, pharmacodynamic; SAR, structure–activity relationship; MOPED, mouse pharmacodynamic erythropoietin determination; POC, proof-of-concept; TMHD, 1,1,6,6-tetramethyl-3,5-heptadione; MED, minimal efficacious dose; NOEL, no observable effect level; PPB, plasma protein binding; LMs, liver microsomes; AE, adverse effect; NMP, N-methylmorpholine; DMF, N,N-dimethylformamide; LiHMDS, lithium bis(trimethylsilyl)amide; DME, dimethoxyethane; PXR, pregnane X receptor; CYP, cytochrome P450; Cav1.2, calcium channel 1.2; PPB, plasma–protein binding; VEGF, vascular endothelial growth factor; RP, reversed phase; HPLC, high-pressure liquid chromatography

■ REFERENCES

- (1) (a) Vilayur, E.; Harris, D. C. H. Emerging therapies for chronic kidney disease: what is their role? *Nature Rev. Nephrol.* **2009**, *5*, 375–383. (b) Kuro-o, M. Klotho in chronic kidney disease—What's new? *Nephrol., Dial., Transplant.* **2009**, *24*, 1705–1708.
- (2) Littlewood, T. J.; Collins, G. P. Pharmacotherapy of anemia in cancer patients. *Expert Rev. Clin. Pharm.* **2008**, *1*, 307–317.
- (3) (a) Cavill, I.; Auerbach, M.; Bailie, G. R.; Barrett-Lee, P.; Beguin, Y.; Kaltwasser, P.; Littlewood, T.; Macdougall, I. C.; Wilson, K. Iron and the anaemia of chronic disease: a review and strategic recommendations. *Curr. Med. Res. Opin.* **2006**, *22*, 731–737. (b) Weiss, G.; Goodnough, L. T. Anemia of chronic disease. *N. Engl. J. Med.* **2005**, *352*, 1011–1023. (c) Minamishima, Y. K.; Kaelin, W. G. Jr. Reactivation of Hepatic EPO Synthesis in Mice After PHD Loss. *Science* **2010**, *329*, 407.
- (4) (a) Percy, M. J.; Zhao, Q.; Flores, A.; Harrison, C.; Lappin, T. R. J.; Maxwell, P. H.; McMullin, M. F.; Lee, F. S. A family with erythrocytosis establishes a role for prolyl hydroxylase domain protein 2 in oxygen homeostasis. *Proc. Natl Acad. Sci. U.S.A.* **2006**, *103*, 654–659. (b) Minamishima, Y. A.; Moslehi, J.; Bardeesy, N.; Cullen, D.; Bronson, R. T.; Kaelin, W. G. Jr. Somatic inactivation of the PHD2 prolyl hydroxylase causes polycythemia and congestive heart failure. *Blood* **2008**, *111*, 3236–3244.
- (5) Chang, Z. Y.; Chiang, C. H.; Lu, D.-W.; Yeh, M.-K. Erythropoiesis-stimulating protein delivery in providing erythropoiesis and neuroprotection. *Expert Opin. Drug Delivery* **2008**, *5*, 1313–1321.
- (6) Cornes, P.; Coiffier, B.; Zambrowski, J.-J. Erythropoietic therapy for the treatment of anemia in patients with cancer: a valuable clinical and economic option. *Curr. Med. Res. Opin.* **2007**, *23*, 357–368.
- (7) (a) Boulahbel, H.; Duran, R. V.; Gottlieb, E. Prolyl hydroxylases as regulators of cell metabolism. *Biochem. Soc. Trans.* **2009**, *37*, 291–294. (b) Rocha, S. Gene regulation under low oxygen: holding your breath for transcription. *Trends Biochem. Sci.* **2007**, *32*, 389–397.
- (8) (a) Provenzano, R. FG-2216, A Novel Oral HIF-PHI, Stimulates Erythropoiesis and Increases Hemoglobin Concentration in Patients with Non-Dialysis CKD. National Kidney Foundation Spring Clinical Meetings 08, Dallas, TX, April 3–6, 2008, Abstract 120. (b) Persons, D. A. A pill for some anemias? *Blood* **2007**, *110*, 1709.
- (9) Another example of small molecule PHDi preclinical effort has been recently disclosed: (a) Barrett, T. D.; Palomino, H. L.; Brondstetter, T. I.; Kanelakis, K. C.; Wu, X.; Haug, P. V.; Yan, W.; Young, A.; Hua, H.; Hart, J. C.; Tran, D.-T.; Venkatesan, H.; Rosen, M. D.; Peltier, H. M.; Sepassi, K.; Rizzolio, M. C.; Bembenek, S. D.; Mirzadegan, T.; Rabinowitz, M. H.; Shankley, N. P. Pharmacological characterization of 1-(5-chloro-6-(trifluoromethoxy)-1H-benzimidazol-2-yl)-1H-pyrazole-4-carboxylic acid (JNJ-42041935), a potent and selective hypoxia-inducible factor prolyl hydroxylase inhibitor. *Mol. Pharmacol.* **2011**, *79*, 910–920. (b) Rosen, M. D.; Venkatesan, H.; Peltier, H. M.; Bembenek, S. D.; Kanelakis, K. C.; Zhao, L. X.; Leonard, B. E.; Hocutt, F. M.; Wu, X.; Palomino, H. L.; Brondstetter, T. I.; Haug, P. V.; Cagnon, L.; Yan, W.; Liotta, L. A.; Young, A.; Mirzadegan, T.; Shankley, N. P.; Barrett, T. D.; Rabinowitz, M. H.; Benzimidazole-2-pyrazole, H. I. F. Prolyl 4-Hydroxylase Inhibitors as Oral Erythropoietin Secretagogues. *ACS Med. Chem. Lett.* **2010**, *1*, 526–529.
- (10) For exceptional reviews, see (a) Chowdhury, R.; Hardy, A.; Schofield, C. J. The human oxygen sensing machinery and its manipulation. *Chem. Soc. Rev.* **2008**, *37*, 1308–1319. (b) Yan, L.; Colandrea, V. J.; Hale, J. J. Prolyl hydroxylase domaincontaining protein inhibitors as stabilizers of hypoxia-inducible factor: small molecule-based therapeutics for anemia. *Expert Opin. Ther. Pat.* **2010**, *20*, 1219–1245. (c) Rabinowitz, M. H.; Barrett, T. D.; Rosen, M. D.; Venkatesan, H. Inhibitors of HIF prolyl hydroxylases. *Annu. Rev. Med. Chem.* **2010**, *45*, 23–139. (d) Muchnik, E.; Kaplan, J. HIF prolyl hydroxylase inhibitors for anemia. *Expert Opin. Invest. Drugs* **2011**, *20*, 645–656.
- (11) (a) Hewitson, K. S.; Schofield, C. J.; Ratcliffe, P. J. Hypoxia-inducible factor prolyl-hydroxylase: purification and assays of PHD2. *Methods Enzym.* **2007**, *435*, 25–42. (b) McDonough, M. A.; Li, V.; Flashman, E.; Chowdhury, R.; Mohr, C.; Lienard, B. M. R.; Zondlo, J.; Oldham, N. J.; Clifton, I. J.; Lewis, J.; McNeill, L. A.; Kurzeja, R. J. M.; Hewitson, K. S.; Yang, E.; Jordan, S.; Syed, R. S.; Schofield, C. J. Cellular oxygen sensing: crystal structure of hypoxia-inducible factor prolyl hydroxylase (PHD2). *Proc. Natl. Acad. Sci. U.S.A.* **2006**, *103*, 9814–9819.
- (12) Annis, D. A.; Athanasopoulos, J.; Curran, P. J.; Felsch, J. S.; Kalghatgi, K.; Lee, W. H.; Nash, H. M.; Orminati, J. P. A.; Rosner, K. E.; Shipps, G. W.; Thaddupathy, G. R. A.; Tyler, A. N.; Vilenchik, L.; Wagner, C. R.; Wintner, E. A. An affinity selection–mass spectrometry method for the identification of small molecule ligands from self-encoded combinatorial libraries. Discovery of a novel antagonist of E. coli dihydrofolate reductase. *Int. J. Mass Spectrom.* **2004**, *238*, 77–83.
- (13) For a detailed description of bioassays, refer to the Experimental Section and Supporting Information.
- (14) Clements, M. J.; Debenham, J. S.; Walsh, T.; Hale, J. J. Unpublished; manuscript in preparation.
- (15) While introduction of the hydroxypyrimidine substituent certainly played a role in the enhancement of the PK properties of **4f**, it remains unclear whether a secondary interaction of the hydroxypyrimidine substituent with the enzyme might have contributed to the observed PD enhancement. It is noteworthy however, that in silico modeling of the enzyme interaction with **4f** vs **5** suggested orthogonal binding modes with respect to the hydroxypyrimidine subunit.
- (16) Initial conditions for this transformation used for the first synthesis of **6a** were analogous to step b1 in Scheme of Table 1: ArI, CuI, MeNHCH₂CH₂NHMe, dioxane.
- (17) (a) Berritt, S.; Goble, S. D.; Tudge, M. T.; Conway, D.; Dreher, S. D. Minimizing the cost of organic chemistry experimentation: low-barrier microscale high-throughput experimentation. 240th ACS National Meeting, Boston, MA, August 22–26, 2010, ORGN-1054. (b) Dreher, S. D. Low-barrier high-throughput experimentation tools for efficient chemistry development. 240th ACS National Meeting, Boston, MA, August 22–26, 2010, ORGN-522. (c) Vachal, P.; Sun, Y. Merck catalysis needs for drug discovery, development, and commercialization. 242nd ACS National Meeting, Denver, CO, August 28–September 1, 2011, ORGN-2.
- (18) Several N-alkyl, N-acyl, and urea derivatives of **6** were prepared. While many exhibited promising in vitro binding, none proved efficacious in vivo and the PK profile was generally suboptimal.
- (19) Mass Spectrometer: Micromass ZQ single quadrupole, electrospray positive ionization, full scan mode (150–750 amu in 0.5s).

HPLC: Agilent 1100, binary pump. DAD UV detector: hardware/software Waters/Micromass MassLynx 4.0. Column: Waters Xterra, 2.1 mm width, 20 mm length, 3.5 μ m packing material. Runtime: 4 min. Flow rate: 1.0 mL /min. Mobile phase A = water + 0.05% TFA, B = acetonitrile + 0.05% TFA. Gradient: time/%A/%B: 0.00/95/05, 3.00/2/98, 3.25/2/98, 3.26/95/5, 4.00/95/5.

(20) Chambers, M. S.; Baker, R.; Billington, D. C.; Knight, A. K.; Middlemiss, D. N.; Wong, E.H. F. Spiropiperidines as high-affinity, selective σ ligands. *J. Med. Chem.* **1992**, *35*, 2033–9.

(21) (a) Sarges, R.; Schnur, R. C.; Belletire, J. L.; Peterson, M. J. Spirohydantoin aldose reductase inhibitors. *J. Med. Chem.* **1988**, *31*, 230–43. (b) Courtoison, J. C.; Coudert, P.; Couquelet, J.; Tronche, P.; Jonadet, M.; Bastide, P. Synthesis and pharmacological testing of some spirohydantoins: relation to conformation. *Farmaco* **1988**, *43*, 153–60.

(22) Tan, S. A Modular Polycistronic Expression System for Overexpressing Protein Complexes in *Escherichia coli*. *Protein Expression Purif.* **2001**, *21*, 224–234.